

Luminescence of Eu^{2+} in Host Lattices with Three Alkaline Earth Ions in a Row

S. H. M. Poort¹, J. W. H. van Krevel, R. Stomphorst, A. P. Vink, and G. Blasse

Debye Institute, Utrecht University, P.O. Box 80 000, 3508 TA Utrecht, The Netherlands

Received August 16, 1995; in revised form January 12, 1996; accepted January 18, 1996

The luminescence of Eu^{2+} in $\text{Sr}_3(\text{PO}_4)_2:\text{Eu}^{2+}$, $\text{Ba}_3(\text{PO}_4)_2:\text{Eu}^{2+}$, $\text{Ba}_2\text{Mg}(\text{B}_3\text{O}_6)_2:\text{Eu}^{2+}$, and $\text{Ba}_2\text{Ca}(\text{B}_3\text{O}_6)_2:\text{Eu}^{2+}$ has been studied. In these structures there are rows of three (large) cations. Emission is observed from Eu^{2+} on the central and the terminal sites in these rows, the longer wavelength emission originating from Eu^{2+} on the central site. This assignment is confirmed by measuring the intensity ratios of the emission bands. It fits a model proposed earlier. © 1996 Academic Press, Inc.

INTRODUCTION

The luminescence of divalent europium has been studied intensively and is applied in fluorescent lighting and in X-ray storage phosphors, but is still not completely understood (1, 2). Therefore Eu^{2+} remains an intriguing ion to study. The emission and absorption spectra of Eu^{2+} usually consist of broad bands due to transitions between the $^8\text{S}_{7/2}$ ($4f^7$) ground state and the crystal field components of the $4f^6 5d$ excited state configuration. The emission varies from ultraviolet to red, depending on the host lattice. In addition to covalency, the size of the cation, and the strength of the crystal field, the emission of Eu^{2+} seems also to be influenced by another effect. In $\text{BaAl}_2\text{O}_4:\text{Eu}^{2+}$ and $\text{SrAl}_2\text{O}_4:\text{Eu}^{2+}$ a green Eu^{2+} luminescence is observed. To explain this long-wavelength Eu^{2+} emission we proposed the following model. In BaAl_2O_4 and SrAl_2O_4 the barium and strontium ions form linear chains in the lattice. A divalent europium ion in these chains experiences, in addition to the negative charges of the nearest anion neighbors, positive charges due to cation neighbors in the chain direction. The positive charges can orient one d orbital preferentially. This will lower its energy and therefore result in a Eu^{2+} emission at longer wavelengths (3). Here we report a study on host lattices with short chains.

The compounds $\alpha\text{-Sr}_3(\text{PO}_4)_2$ and $\alpha\text{-Ba}_3(\text{PO}_4)_2$ are isostructural with $\text{Ba}_3(\text{VO}_4)_2$ (4, 5). In this type of structure there are two different sites available for the divalent cat-

ions, one site occurring twice more frequently than the other. The most frequently occurring site is coordinated by 10 oxygen ions, the other by 12 oxygen ions. The structure of $\text{Ba}_2\text{Mg}(\text{B}_3\text{O}_6)_2$ and $\text{Ba}_2\text{Ca}(\text{B}_3\text{O}_6)_2$ is built from nearly planar B_3O_6 rings, and is related to the high temperature (β) form of BaB_2O_4 (6). The barium sites are coordinated by 9 oxygen ions and the coordination of the calcium site is octahedral.

These crystal structures have in common that three (large) cations are arranged in a linear row. This implies that there are two different sites available for Eu^{2+} : one site at the end, the other in the center. According to our model the latter should emit at longer wavelengths.

EXPERIMENTAL

Preparation

The measurements were performed on powder samples with composition $\text{Sr}_3(\text{PO}_4)_2:\text{Eu}^{2+}$, $\text{Ba}_3(\text{PO}_4)_2:\text{Eu}^{2+}$, $\text{Ba}_2\text{Mg}(\text{B}_3\text{O}_6)_2:\text{Eu}^{2+}$, and $\text{Ba}_2\text{Ca}(\text{B}_3\text{O}_6)_2:\text{Eu}^{2+}$. The Eu^{2+} mole fractions were 1×10^{-2} . The starting materials were high-purity BaCO_3 (Philips Maarheeze), SrCO_3 (Philips Maarheeze), CaCO_3 (Merck), MgO (Merck), H_3BO_3 (Merck), $(\text{NH}_4)_2\text{HPO}_4$ (Merck), and Eu_2O_3 (Highways Int., 99.99%). All samples were prepared by solid state reactions. Stoichiometric amounts of the starting materials were thoroughly mixed in a planetary ball mill and subsequently fired in a reducing atmosphere (25% H_2 / 75% N_2). $\text{Sr}_3(\text{PO}_4)_2:\text{Eu}^{2+}$ and $\text{Ba}_3(\text{PO}_4)_2:\text{Eu}^{2+}$ were synthesized by firing twice at 900 and 1200°C for 2 to 3 h. To synthesize $\text{Ba}_2\text{Ca}(\text{B}_3\text{O}_6)_2:\text{Eu}^{2+}$ and $\text{Ba}_2\text{Mg}(\text{B}_3\text{O}_6)_2:\text{Eu}^{2+}$ three firing steps at temperatures ranging from 800 to 850°C for 12 to 20 h were necessary. The samples were confirmed to be single phase by X-ray powder diffraction using $\text{CuK}\alpha$ radiation.

Optical Measurements

Diffuse reflection spectra were recorded on a Perkin-Elmer Lambda 7 UV/Vis spectrophotometer. BaSO_4 was

¹ To whom correspondence should be addressed.

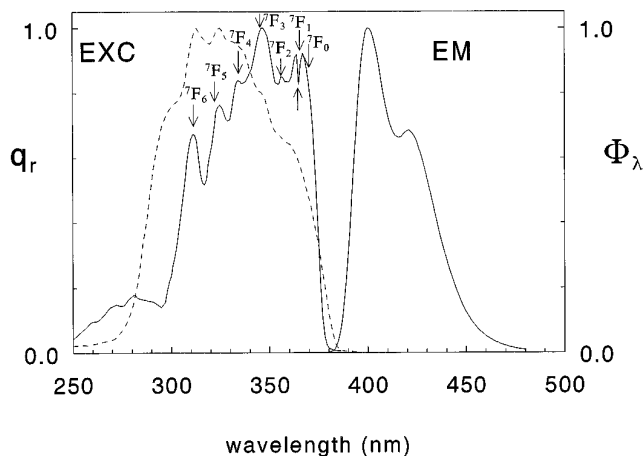


FIG. 1. Excitation spectra (EXC) of $\text{Sr}_3(\text{PO}_4)_2:1\% \text{Eu}^{2+}$ at 4.2 K (solid curve: $\lambda_{\text{em}} = 400$ nm, dashed curve: $\lambda_{\text{em}} = 420$ nm). Emission spectrum (EM) of $\text{Sr}_3(\text{PO}_4)_2:1\% \text{Eu}^{2+}$ at 4.2 K ($\lambda_{\text{exc}} = 350$ nm). Fano antiresonance is indicated by an arrow (\uparrow). The relative positions of the 7F_J levels calculated from the theoretical splitting are also indicated (see also text).

used as a reference. The luminescence spectra were recorded on a SPEX Fluorolog spectrofluorometer equipped with two double-grating 0.22 m SPEX 1680-monochromators and a xenon lamp as an excitation source. Measurements at 4.2 K and temperature dependent measurements up to room temperature were performed with the SPEX spectrofluorometer equipped with an Oxford Instruments liquid helium flow cryostat. The excitation spectra are not corrected for the xenon lamp intensity. This would raise the spectra on the shorter wavelength side.

RESULTS

$\text{Sr}_3(\text{PO}_4)_2:\text{Eu}^{2+}$ and $\text{Ba}_3(\text{PO}_4)_2:\text{Eu}^{2+}$

The emission spectrum of $\text{Sr}_3(\text{PO}_4)_2:\text{Eu}^{2+}$ at 4.2 K shows two maxima, at 400 and 425 nm (Fig. 1). At room temperature the intensity of both emission bands is about 85 to 90% of the intensity at 4.2 K. In the emission spectrum at room temperature the two maxima can be distinguished less clearly than in the spectrum at 4.2 K due to broadening of both bands. The excitation spectrum at room temperature is broad and structureless and consistent with the reflection spectrum of $\text{Sr}_3(\text{PO}_4)_2:\text{Eu}^{2+}$. The excitation spectrum at 4.2 K shows structure (Fig. 1). The structure in the longer wavelength part of the excitation band can be ascribed to the splitting of the $4f^6$ configuration in the $4f^6 5d$ excited state into seven 7F_J levels (7). The agreement between the theoretical splitting of the $4f^6$ configuration, which is well known from Eu^{3+} (8, 9), and the observed splitting is satisfying. The arrows in Fig. 1 give the relative positions of the 7F_J levels calculated from the theoretical

splitting of the 7F_J levels. The sharp dip at 363 nm is ascribed to Fano antiresonance due to interaction between the $4f^7$ states and the $4f^6 5d$ states (10). As can be seen in Fig. 1, the excitation spectra of $\text{Sr}_3(\text{PO}_4)_2:\text{Eu}^{2+}$ are dependent on the emission wavelength. By exciting at 4.2 K with broad excitation slits at several positions in the region from 300 to 370 nm, both Eu^{2+} sites will be excited equally, and the ratio of the intensities of the emission bands will represent the distribution of Eu^{2+} on both strontium sites. The intensity of the shorter wavelength emission band turned out to be twice as high as the intensity of the longer wavelength emission band. The observed fine structure in the excitation spectra makes an accurate determination of the Stokes shifts possible. For the emission at 400 and 425 nm the Stokes shifts are 2000 and 3300 cm^{-1} , respectively (Table 1).

In contrast to $\text{Sr}_3(\text{PO}_4)_2:\text{Eu}^{2+}$, the emission spectrum of $\text{Ba}_3(\text{PO}_4)_2:\text{Eu}^{2+}$ at 4.2 K shows a broad band at about 410 nm. On an energy scale it can be seen that the emission band is built up from two Gaussian bands. The positions of these emission bands and also the temperature dependence are comparable to those of $\text{Sr}_3(\text{PO}_4)_2:\text{Eu}^{2+}$. Because the excitation spectra of $\text{Ba}_3(\text{PO}_4)_2:\text{Eu}^{2+}$ at room temperature and 4.2 K are broad and structureless, only a rough estimation of the Stokes shifts can be made. No clear dependence of the excitation spectra on the emission wavelength is observed. In Table 1 the results on the luminescence of Eu^{2+} in $\text{Ba}_3(\text{PO}_4)_2$ are summarized.

$\text{Ba}_2\text{Mg}(\text{B}_3\text{O}_6)_2:\text{Eu}^{2+}$ and $\text{Ba}_2\text{Ca}(\text{B}_3\text{O}_6)_2:\text{Eu}^{2+}$

The emission spectrum of $\text{Ba}_2\text{Mg}(\text{B}_3\text{O}_6)_2:\text{Eu}^{2+}$ at 4.2 K consists of an emission band at 425 nm and a less intense emission band at longer wavelengths (Fig. 2). On an energy

TABLE 1
Luminescence Properties of Eu^{2+} -activated $\text{Sr}_3(\text{PO}_4)_2$,
 $\text{Ba}_3(\text{PO}_4)_2$, $\text{Ba}_2\text{Mg}(\text{B}_3\text{O}_6)_2$, and $\text{Ba}_2\text{Ca}(\text{B}_3\text{O}_6)_2$

Composition	Emission maxima at 4.2 K (nm)	$T_{1/2}^a$ (K)	Stokes shift (cm^{-1})
$\text{Sr}_3(\text{PO}_4)_2:\text{Eu}^{2+}$	400	>300	2000
	425	>300	3300
$\text{Ba}_3(\text{PO}_4)_2:\text{Eu}^{2+}$	405	>300	2000
	425	>300	3000
$\text{Ba}_2\text{Mg}(\text{B}_3\text{O}_6)_2:\text{Eu}^{2+}$	425	120	3500
	475	170	5000
$\text{Ba}_2\text{Ca}(\text{B}_3\text{O}_6)_2:\text{Eu}^{2+}$	450	260	4500
	495	230	6000

^a Temperature at which half of the emission intensity at 4.2 K is reached.

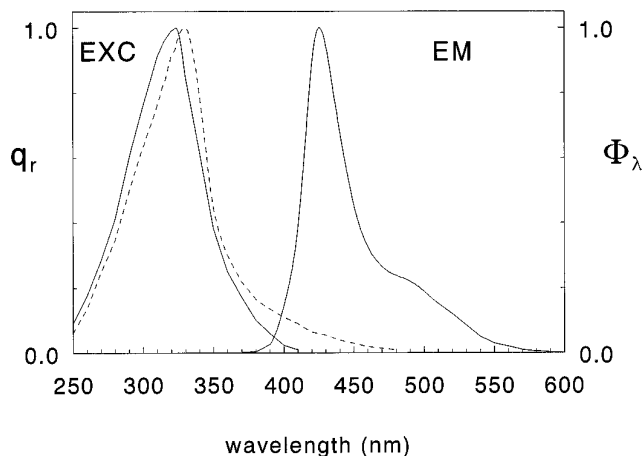


FIG. 2. Excitation spectra (EXC) of $\text{Ba}_2\text{Mg}(\text{B}_3\text{O}_6)_2:1\% \text{Eu}^{2+}$ at 4.2 K (solid curve: $\lambda_{\text{em}} = 425 \text{ nm}$, dashed curve: $\lambda_{\text{em}} = 520 \text{ nm}$). Emission spectrum (EM) of $\text{Ba}_2\text{Mg}(\text{B}_3\text{O}_6)_2:1\% \text{Eu}^{2+}$ at 4.2 K ($\lambda_{\text{exc}} = 325 \text{ nm}$).

scale the emission band can be separated into two Gaussian bands with maxima at about $21,000$ and $23,500 \text{ cm}^{-1}$. At room temperature the intensities of both emission bands are comparable. Because they are also broader, the emission bands are not as clearly observable as in the emission spectrum at 4.2 K. Both emissions are much stronger temperature dependent than in $\text{Sr}_3(\text{PO}_4)_2:\text{Eu}^{2+}$ and $\text{Ba}_3(\text{PO}_4)_2:\text{Eu}^{2+}$. The temperature at which half of the emission intensity at 4.2 K is reached is 120 K for the emission at 425 nm and 170 K for the emission at 475 nm. Similar to $\text{Ba}_3(\text{PO}_4)_2:\text{Eu}^{2+}$, the excitation spectra at 4.2 K are broad and do not show fine structure (Fig. 2). Therefore, only a rough estimation of the Stokes shifts of about 3500 and 5000 cm^{-1} for the emissions at 425 and 475 nm, respectively, can be made (Table 1).

The emission spectrum of $\text{Ba}_2\text{Ca}(\text{B}_3\text{O}_6)_2:\text{Eu}^{2+}$ at 4.2 K shows a broad emission band at about 450 nm. This emission band is broader than the emission band of $\text{Ba}_2\text{Mg}(\text{B}_3\text{O}_6)_2:\text{Eu}^{2+}$ and only on an energy scale it is clear that it consists of two Gaussian bands. Because the emission bands are strongly overlapping, the inaccuracy in the values for the temperature dependence of the intensity of both emission bands will be considerable. At 4.2 K the intensity of the shorter wavelength emission is about 1.5 to 2 times higher than that of the longer wavelength emission. This is different from the intensity ratio of the Eu^{2+} emissions in $\text{Ba}_2\text{Mg}(\text{B}_3\text{O}_6)_2:\text{Eu}^{2+}$ (Fig. 2). Similar to $\text{Ba}_2\text{Mg}(\text{B}_3\text{O}_6)_2:\text{Eu}^{2+}$, the excitation spectra at room temperature and 4.2 K are broad and structureless and dependent on the emission wavelength. When the emission wavelength is chosen on the longer wavelength side of the emission band, the excitation spectrum is shifted to longer wavelengths. In Table 1 the results on the luminescence of Eu^{2+} in $\text{Ba}_2\text{Ca}(\text{B}_3\text{O}_6)_2$ are summarized.

DISCUSSION

$\text{Sr}_3(\text{PO}_4)_2:\text{Eu}^{2+}$ and $\text{Ba}_3(\text{PO}_4)_2:\text{Eu}^{2+}$

A blue Eu^{2+} emission for $\text{Sr}_3(\text{PO}_4)_2:\text{Eu}^{2+}$ has been reported earlier by Nazarova (11) and Gorbacheva (12). However, they observed only one Eu^{2+} emission, whereas emission from Eu^{2+} on both strontium sites is observed by us. Also in $\text{Ba}_3(\text{PO}_4)_2:\text{Eu}^{2+}$ emission from Eu^{2+} on both barium sites present in the lattice is observed. Based on the model proposed earlier (3), Eu^{2+} on the central position is expected to have its emission at longer wavelengths than Eu^{2+} on the terminal positions in the linear row. This is due to the fact, that the Sr^{2+} or Ba^{2+} ions at the terminal positions experience, in addition to the negative charges of the nearest anion neighbors, a positively charged ion on only one side, whereas the central ion experiences positive charges on both sides. These positive charges can orient one d orbital preferentially and therefore lower its energy which will result in a Eu^{2+} emission at longer wavelengths. Because Eu^{2+} is not expected to have a preference for one of the two available sites, it will be possible to determine which Eu^{2+} emission is due to which Eu^{2+} from the intensity ratio of both emission bands. These measurements were done for $\text{Sr}_3(\text{PO}_4)_2:\text{Eu}^{2+}$, because in the emission spectra at 4.2 K both emission bands can be discriminated more accurately than in the emission spectra of $\text{Ba}_3(\text{PO}_4)_2:\text{Eu}^{2+}$. As the intensity of the shorter wavelength emission band turned out to be twice as high as the intensity of the longer wavelength emission band, it can be concluded that the longer wavelength emission is due to Eu^{2+} on the central position in the linear rows of strontium ions. This is in accordance with our model.

$\text{Ba}_2\text{Mg}(\text{B}_3\text{O}_6)_2:\text{Eu}^{2+}$ and $\text{Ba}_2\text{Ca}(\text{B}_3\text{O}_6)_2:\text{Eu}^{2+}$

In these lattices there are linear rows of Ba^{2+} , Mg^{2+} , or Ca^{2+} , and again Ba^{2+} . An important difference between this situation and that in $\text{Sr}_3(\text{PO}_4)_2:\text{Eu}^{2+}$ and $\text{Ba}_3(\text{PO}_4)_2:\text{Eu}^{2+}$ is, that in these compounds a divalent europium ion is expected to prefer the barium site above the magnesium and even above the calcium site because of the ionic radii (13). Similar to $\text{Sr}_3(\text{PO}_4)_2:\text{Eu}^{2+}$ and $\text{Ba}_3(\text{PO}_4)_2:\text{Eu}^{2+}$, Eu^{2+} on the terminal barium sites is expected to have its emission at shorter wavelengths than Eu^{2+} on the central magnesium or calcium sites. Because of the site preference of Eu^{2+} based on ionic radii, the emission at shorter wavelengths is expected to have the higher intensity. At 4.2 K this is indeed observed for $\text{Ba}_2\text{Mg}(\text{B}_3\text{O}_6)_2:\text{Eu}^{2+}$ (Fig. 2). However, in $\text{Ba}_2\text{Ca}(\text{B}_3\text{O}_6)_2:\text{Eu}^{2+}$ the intensity of the shorter wavelength emission is higher than expected based on ionic radii. Partly, this can be due to the fact that Ca^{2+} is larger than Mg^{2+} and to disorder of barium and calcium ions.

The latter would also explain why the emission bands are broader than those of $\text{Ba}_2\text{Mg}(\text{B}_3\text{O}_6)_2:\text{Eu}^{2+}$ at 4.2 K. Another effect will be energy transfer. Since allowed electric-dipole transitions are involved in the case of Eu^{2+} , the value of the critical transfer distance (R_c) can be calculated from (14)

$$R_c = 0.36 \times 10^{28} \frac{4.8 \times 10^{-16} \cdot P}{E^4} \text{S.O.}$$

Here, P is the oscillator strength of the involved absorption transition of the Eu^{2+} ion, E the energy of maximum spectral overlap, and S.O. the spectral overlap integral. For P a value of 10^{-2} for the broad $4f^7 \rightarrow 4f^6 5d$ absorption band is taken (15). E and S.O. can be derived from the spectral data. The calculated value of R_c for the energy transfer between inequivalent Eu^{2+} ions in $\text{Ba}_2\text{Ca}(\text{B}_3\text{O}_6)_2:\text{Eu}^{2+}$ is 17 Å. In $\text{Ba}_2\text{Mg}(\text{B}_3\text{O}_6)_2:\text{Eu}^{2+}$ R_c is 15 Å. These calculations suffer from a large inaccuracy in the S.O. due to the broad structureless absorption bands. These values of R_c can be compared to values of R_c found for Eu^{2+} in other lattices (15), and indicate that energy transfer between the different Eu^{2+} ions in both compounds will be efficient. Also, the stronger temperature dependence of the shorter wavelength emission in $\text{Ba}_2\text{Mg}(\text{B}_3\text{O}_6)_2:\text{Eu}^{2+}$ is, of course, due to the enhanced energy transfer at higher temperatures.

From these results we conclude that the Eu^{2+} ion occupies preferentially the terminal sites in the row where they have, as predicted, the shorter wavelength emission. However, part of the Eu^{2+} ions occupies the central site in the row where they have the longer wavelength emission.

In $\text{Sr}_3(\text{PO}_4)_2:\text{Eu}^{2+}$ and $\text{Ba}_3(\text{PO}_4)_2:\text{Eu}^{2+}$ the Eu^{2+} emission bands are at shorter wavelengths than in $\text{Ba}_2\text{Mg}(\text{B}_3\text{O}_6)_2:\text{Eu}^{2+}$ and $\text{Ba}_2\text{Ca}(\text{B}_3\text{O}_6)_2:\text{Eu}^{2+}$ (Table 1). Also, the energy difference between the emissions from Eu^{2+} on both sites in the phosphates is smaller than in the borates, viz. about 1300 cm^{-1} and about 2200 cm^{-1} , respectively. In addition to the influence of the size and the coordination of the cation, this can be explained considering the distances between the cations in the rows. In $\text{Sr}_3(\text{PO}_4)_2:\text{Eu}^{2+}$ and $\text{Ba}_3(\text{PO}_4)_2:\text{Eu}^{2+}$ the distances from the central to the terminal strontium or barium ions are 4.1 and 4.3 Å, respectively (4). However, in $\text{Ba}_2\text{Mg}(\text{B}_3\text{O}_6)_2:\text{Eu}^{2+}$ and $\text{Ba}_2\text{Ca}(\text{B}_3\text{O}_6)_2:\text{Eu}^{2+}$ these distances are smaller, viz. 3.5 and 3.7 Å, respectively (6). Because of this, the influence of the positively charged ions on both sides of the central ion

will be larger in the borates than in the phosphates. This means that the preferential orientation of a d orbital will be more favorable in the borates and therefore the Eu^{2+} emission will be at longer wavelengths in $\text{Ba}_2\text{Mg}(\text{B}_3\text{O}_6)_2:\text{Eu}^{2+}$ and $\text{Ba}_2\text{Ca}(\text{B}_3\text{O}_6)_2:\text{Eu}^{2+}$.

CONCLUSIONS

In $\text{Sr}_3(\text{PO}_4)_2:\text{Eu}^{2+}$, $\text{Ba}_3(\text{PO}_4)_2:\text{Eu}^{2+}$, $\text{Ba}_2\text{Mg}(\text{B}_3\text{O}_6)_2:\text{Eu}^{2+}$, and $\text{Ba}_2\text{Ca}(\text{B}_3\text{O}_6)_2:\text{Eu}^{2+}$, Eu^{2+} emission is observed from the two different sites in the lattices, which are available for Eu^{2+} . In these structures there are linear rows of three cations which can be replaced by Eu^{2+} . The longer wavelength emission is due to Eu^{2+} on the central position in the row, because the preferential orientation of a d orbital is more favorable on these sites than on the terminal positions in the row. Because the distances between the cations in the borates are smaller than in the phosphates, this effect is more pronounced in the former compounds. As a consequence, the emission maxima are at longer wavelengths and the energy difference between the Eu^{2+} emissions is larger in the borates.

ACKNOWLEDGMENT

The work described here was supported by the Netherlands Foundation for Chemical Research (SON) with financial aid from the Netherlands Organization for Scientific Research (NWO), the Netherlands Foundation for Technical Research (STW), and Philips Lighting B.V.

REFERENCES

1. G. Blasse and B. C. Grabmaier, "Luminescent Materials," Chap. 6–9. Springer-Verlag, Berlin, 1994.
2. A. Meijerink, Ph.D. Thesis, Utrecht, 1990.
3. S. H. M. Poort, W. P. Blokpoel, and G. Blasse, *Chem. Mater.* **7**, 1547 (1995).
4. W. H. Zachariasen, *Acta Crystallogr.* **1**, 263 (1948).
5. P. Süsse and M. J. Buerger, *Z. Kristallogr.* **131**, 161 (1970).
6. J. Liebertz and R. Frölich, *Z. Kristallogr.* **168**, 293 (1984).
7. F. M. Ryan, W. Lehmann, D. W. Feldman, and J. Murphy, *J. Electrochem. Soc.* **121**, 1475 (1974).
8. N. C. Chang and J. B. Gruber, *J. Chem. Phys.* **41**, 3227 (1964).
9. W. T. Carnall, G. L. Goodman, K. Rajnak, and R. S. Rana, *J. Chem. Phys.* **90**, 3443 (1989).
10. A. Meijerink and G. Blasse, *Phys. Rev. B* **40**, 7288 (1989).
11. V. P. Nazarova, *Bull. Acad. Sci. USSR (Phys. Ser.)* **25**, 322 (1961).
12. N. A. Gorbacheva, *Bull. Acad. Sci. USSR (Phys. Ser.)* **30**, 1586 (1966).
13. R. D. Shannon and C. T. Prewitt, *Acta Crystallogr. B* **25**, 925 (1969).
14. G. Blasse, *Philips Res. Repts.* **24**, 131 (1969).
15. G. Blasse, *J. Solid State Chem.* **62**, 207 (1986).